**Neuroendocrinology Letters** Volume 45 No. 2 2024
ISSN: 0172-780X; ISSN-L: 0172-780X; Electronic/Online ISSN: 2354-4716
*Web of Knowledge / Web of Science:* Neuroendocrinol Lett
*Pub Med / Medline:* Neuro Endocrinol Lett



ORIGINAL ARTICLE

# Rosiglitazone Promotes Microglial Distribution via Activation of PPARγ and CD36 in the ICH Rat Model.

**Qiong Mu[1], Qian He[1], Hailong Zhou[2], Yingning Xu[1], Guofeng Wu[3]**

1 Department of General practice, Affiliated Hospital of Guizhou Medical University, No. 28, Guiyijie Road, Guiyang 550004, Guizhou, China.
2 The Fourth People's Hospital of Guiyang, No. 91, Jiefang West Road, Guiyang 550002. Guizhou, China.
3 Department of emergency, Affiliated Hospital of Guizhou Medical University, No. 28, Guiyi Road, Guiyang 550004, Guizhou, China.

*Correspondence to:* Guofeng Wu
Department of emergency, Affiliated Hospital of Guizhou Medical University, No. 28, Guiyi Road, Guiyang 550004, Guizhou, China
TEL: 13985112789, E-MAIL: gfwu1234@126.com

*Submitted: 2023-12-14 Accepted: 2024-02-22 Published online: 2024-03-28*

*Key words:* **intracerebral hemorrhage; rosiglitazone; PPARγ; microglia; CD36**

Neuroendocrinol Lett 2024; **45**(2):96–106 **PMID:** 38583188 NEL450224A04 

## Abstract

**OBJECTIVES:** Intracerebral hemorrhage (ICH) is a serious public health problem with high mortality and morbidity. The current study aims to investigate the effects of rosiglitazone on the microglial distribution and the expression of PPARγ and CD36 in the ICH rat model.

**METHODS NEW:** Sprague-Dawley male rats (n=116) were randomly divided into four groups: control, ICH, rosiglitazone, and PPARγ antagonist (GW9662). Hematoxylin-eosin staining was used to observe the brain edema in the ICH rat model. The effect of rosiglitazone on the expression of OX-42, a microglial marker, was evaluated by immunohistochemistry. Immunohistochemistry, quantitative real-time PCR, and western blot were utilized to assess the role of rosiglitazone in the expression of PPARγ and CD36.

**RESULTS:** ICH rats exhibited a remarkable brain edema at 72 h. OX-42 expression was significantly increased in brain tissues of ICH rats. Rosiglitazone remarkably promoted the OX-42 expression in ICH rats, whereas GW9662 suppressed OX-42 expression. In addition, immunohistochemistry analysis showed that rosiglitazone markedly enhanced the expression of PPARγ and CD36 in brain tissues around the hematoma in ICH rats, while GW9662 inhibited their expression in ICH rats. Moreover, rosiglitazone significantly promoted the mRNA and protein expression of PPARγ and CD36 in the brain tissues of ICH rats, while GW9662 showed the opposite trend.

**CONCLUSION:** Rosiglitazone may improve microglial distribution via promoting the expression of PPARγ and CD36 around the hematoma in the ICH rat model, which may provide effective therapeutic targets for the treatment of ICH.

## INTRODUCTION

Intracerebral hemorrhage (ICH), a life-threatening type of stroke, is one of the leading causes of death and injury worldwide (Duan *et al.* 2016). Intracerebral haemorrhage constituted 27.9% of all new strokes in 2019. The absolute number of ICH globally increased by 43.0% (41.0-45.0) from 1990 to 2019 and deaths increased by 37.0% (22.0-51.0) (Kisa *et al.* 2021). The pathology of ICH is very complex, including primary and secondary brain injury (de Oliveira 2020). Primary brain injury refers to damage to brain tissue caused by hematoma in a few minutes or hours after ICH, which can be reduced by removing the hematoma and removing the occupying effect (Keep *et al.* 2012). Secondary brain injury is caused by hematoma, and oxidative stress, which is induced by inflammation, degradation products of erythrocyte, and ROS released by microglial/macrophage (Lan *et al.* 2017; Qureshi & Qureshi 2018). Secondary brain injury is the key to determine the prognosis of ICH. Timely clearance of red blood cells and release of cytotoxic substances can effectively ameliorate secondary brain injury, thus decreasing the disability rate and mortality of ICH (Qureshi *et al.* 2016). Therefore, it is necessary to understand the pathogenesis of ICH progress for the treatment of ICH.

Microglia, accounting for 10% of all glial cells, are the most important immune effector cells of the central nervous system and exert a vital role in secondary brain injury after ICH (Zhang *et al.* 2017). A previous study reported that microglia are activated after ICH, and recognized and phagocytized red blood cells through CD36, a receptor on the surface of their cell membranes (Jesberger & Richardson 1991). CD36 is a type II scavenger receptor, which can bind to modified lipids on symmetric red cell ghosts or apoptotic neutrophils (Fadok *et al.* 1998). CD36 plays an important role in hematoma absorption. For example, Fang *et al.* examined hematoma absorption in CD36-deficient ICH patients and found that CD36 regulated the hematoma absorption which was remarkably associated with the prognosis of patients (Fang *et al.* 2014). Flores *et al.* discovered that upregulation of CD36 could promote hematoma resolution (Flores *et al.* 2016). Therefore, the protective effect of activated microglia on the central nervous system after ICH may be via upregulation of CD36.

Peroxisome proliferator-activated receptor-gamma (PPARγ) is a transcription factor located in the nuclear membrane (Berger & Moller 2002). The PPARγ agonists include prostaglandin D2, fatty acid, non-steroidal anti-inflammatory drugs, and thiazolidinedione (rosiglitazone and pioglitazone) (Sundararajan *et al.* 2006). PPARγ agonists can reduce secondary brain injury and have a protective effect on nerve cells (Qureshi & Qureshi 2018; Wu *et al.* 2015). A recent study has been shown that PPARγ had a neuro-protective effect by inhibiting tissue inflammation in animal models of cerebral ischemia, cerebral hemorrhage, and spinal cord injury (Qureshi *et al.* 2016). Upregulation of PPARγ promoted hematoma clearance and improved overall prognosis of cerebral hemorrhage in rat models (Wu *et al.* 2016; Han *et al.* 2008). Rosiglitazone is a special activator of PPARγ and has been widely studied in neurology (Fischer *et al.* 2017). In ischemic brain disease, rosiglitazone can lower the inflammatory response and the autophagy of nerve cells (Kollmar *et al.* 2012). Rosiglitazone has also been proven to prevent recurrent stroke and other vascular events in patients with transient ischemia or stroke (Wang *et al.* 2017). However, the mechanism by which rosiglitazone promotes hematoma clearance in ICH rat model remains unknown.

In the present study, an ICH rat model was constructed to investigate the effect of rosiglitazone on microglial distribution. Additionally, the expression of PPARγ and CD36 in ICH rats was detected using immunohistochemistry, western blot and quantitative reverse transcription PCR (qRT-PCR). This study gives us a deep insight into the mechanism by which rosiglitazone regulates the microglial distribution after ICH.

## MATERIALS AND METHODS

### *Animals*

Estrogen has a protective effect on ICH, which reduces the success rate of modeling to some extent (Kirkman *et al.* 2011; Xiao *et al.* 2021). The effect of androgens on ICH is relatively small. Male rats have been selected in many studies (Zhang *et al.* 2021; Zhang *et al.* 2019). Therefore, we used male rats. A total of 116 healthy Sprague-Dawley male rats (each weight about 250-300 g) were procured from the Animal Experimental Center of Guizhou Medical University. Rats were given free access to food and water. All experimental procedures were approved by the Ethical Committee and the Animal Experimental Committee of Affiliated Hospital of Guizhou Medical University.

### *Preparation of the ICH rat model*

The rats were anesthetized with 10% chloral hydrate (350 mg/kg intra-peritoneally) and fixed on a stereotaxic frame to expose the skull and reveal the bregma. A 1.5 mm diameter cranial burr hole was drilled into the skull (coordinates: 1.0 mm anterior to the bregma, 3.5 mm right lateral to the midline). Next, 1 mL of autologous arterial blood was obtained from the central artery of the rat tail and immediately injected into an Eppendorf tube containing anticoagulants. Then, about 50 μL blood was inserted into the burr hole (6 mm deep) using a microinjector. First, 10 μL blood was delivered at a rate of 10 μL/min and the needle was kept stationary for 1 min. Following this, the remaining 40 μL blood was delivered slowly. After 2 min, the needle was slowly withdrawn. After the operation, the

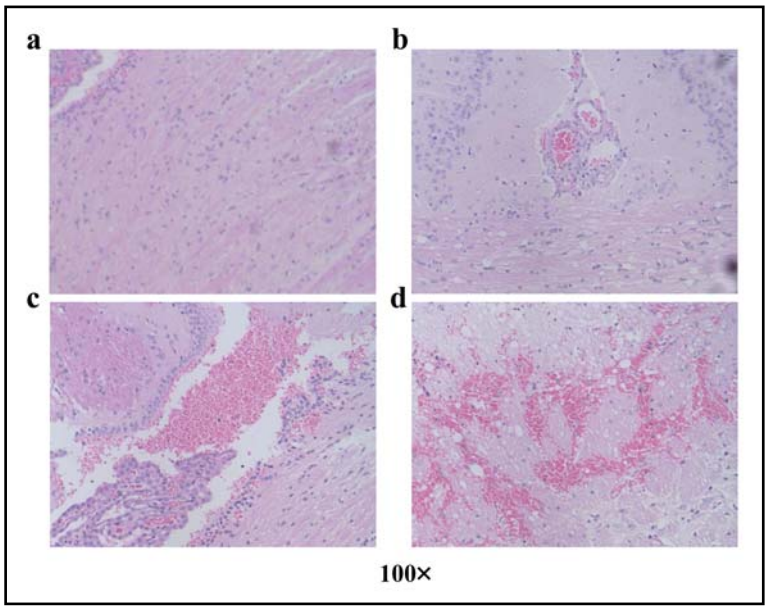


**Fig. 1. HE staining of the brain tissues in the ICH group at different time points was observed under the light microscope.** (a) The morphology of the brain cells was normal at 6 h after modeling. (b) Patchy hemorrhagic foci and edema of surrounding tissues was observed at 24 h after modeling. (c) At 48 h after modeling, massive hemorrhagic foci and infiltration of a large number of inflammatory cells was observed around the hematoma. (d) The tissue edema was the most obvious at 72 h after modeling. The arrow indicates inflammatory cells. Magnification: ×100.

skull hole was sealed with bone wax and wrapped using sterile dressings.

*Experimental groups*

The 116 rats were randomly allocated into 4 groups: control group (n=20), ICH group (n=32), PPARγ agonist group (RSG group, n=32), and PPARγ antagonist group (GW9662 group, n=32). No rats died during the sham-operated procedure and ICH surgery. In the control group, the animals only received the puncture without injection of blood into the brain. In the other three groups, autologous arterial blood taken from the central artery of the rat tail was injected into the basal ganglia to establish the ICH model. The dosage and time points of rosiglitazone was chosen according to the preliminary experiments and relevant references (Yao *et al.* 2015; Sagir *et al.* 2018; Zhao *et al.* 2007). In the RSG group, rats were given rosiglitazone (3 mg/kg) by gavage for 3 days before modeling. Next, the rats were given rosiglitazone by gavage at 1 h after modeling, and then rosiglitazone was given daily until the rats were sacrificed. In the GW9662 group, rats were

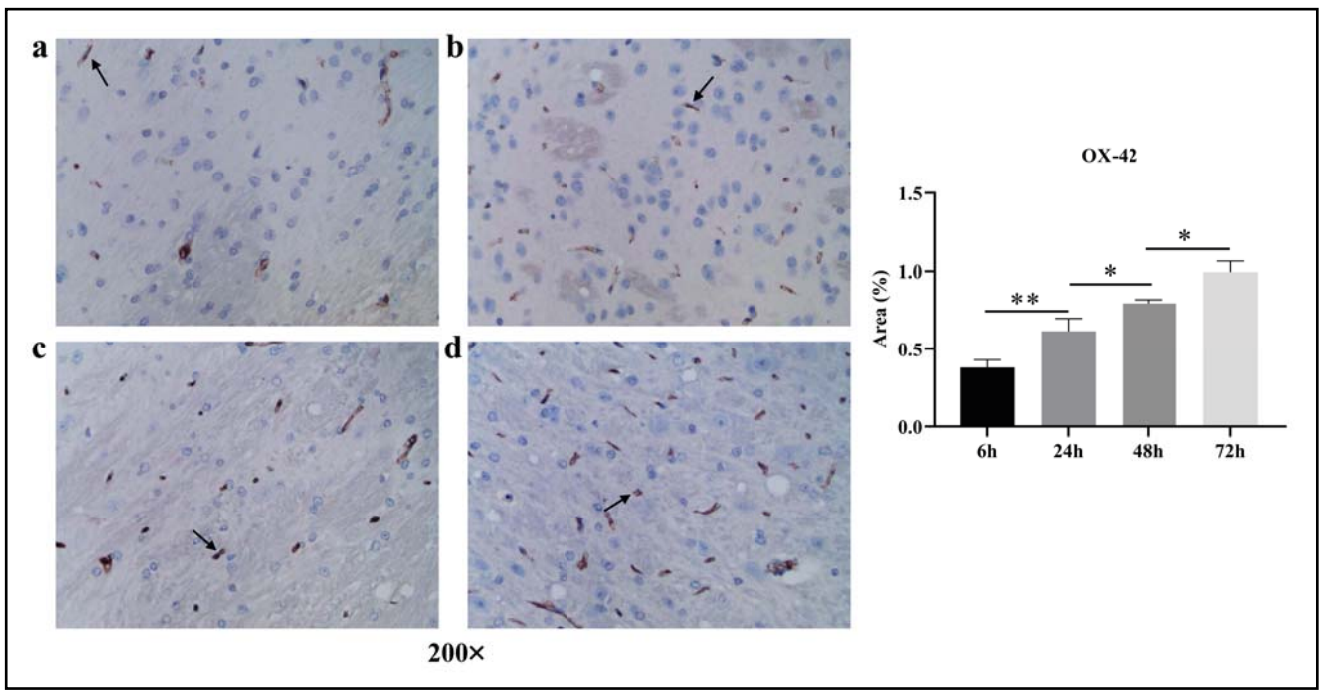


**Fig. 2. Expression of the microglial marker, OX-42, in the tissues around the hematoma was observed under the light microscope at different time points after modeling.** (a) 6 h, (b) 24 h, (c) 48 h and (d) 72 h after modeling. The positive expression of microglia labeled with OX-42 increased with time. The arrow indicates microglia expression. Magnification: ×200. *$p < 0.05$; ** $p < 0.01$.

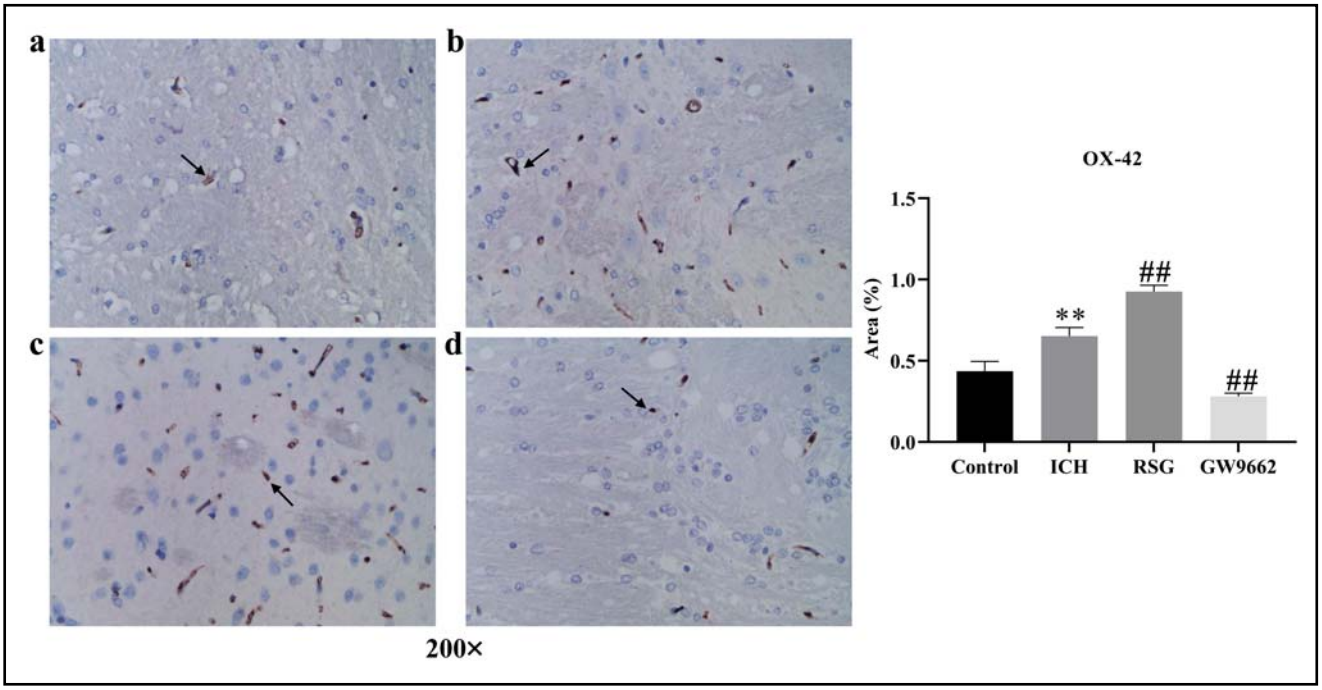


**Fig. 3. Expression of the microglial marker, OX-42, in the tissues around the hematoma of each group 72 h after modeling.** (a) control group, (b) ICH group, (c) RSG group (PPARγ agonist group), (d) GW9662 group (PPARγ antagonist group). The arrow indicates microglia expression. Magnification: ×200. ** $p < 0.01$ versus the control group. ## $p < 0.01$ versus the ICH group.

intra-peritoneally injected with GW9662 (4 mg/kg) -dissolved in 10% dimethylsulfoxide after successful establishment of the ICH model. We selected the time points for testing according to the relevant references (Wang 2010; Fei *et al.* 2019). All groups of rats were sacrificed at 6 h, 24 h, 48 h, and 72 h, and brain tissues were collected for examination.

*Hematoxylin-eosin (HE) staining*

The brain tissues at the lesion side (0.5×0.5×0.5 $cm^3$) were taken for HE staining. The brain tissues were put in 10% formaldehyde solution for tissue fixation, then placed in the embedding box and finally rinsed under running water for 30 min. Then the tissue was embedded in paraffin. The staining process was performed as follows: hematoxylin staining, eosin staining, transparency, and sealing. Finally, images were collected and analyzed.

*Immunohistochemistry*

Brain tissues were put in the oven and baked for 30 min. Brain tissue slides were deparaffinized, dehydrated in alcohol and washed with phosphate buffer saline (PBS) three times. Then, antigen retrieval was performed by boiling the sections in 0.01 M sodium citrate buffer. The sections were blocked with 5% BSA and incubated overnight with rabbit anti-PPARγ (1:200, ab310323, Abcam), rabbit anti-CD36 (1:1000, ab252922, Abcam), and mouse anti-OX-42 (1:500, MA1-21591, Invitrogen) primary antibodies at 4°C followed by incubating with Goat Anti-Rabbit IgG H&L (HRP) secondary antibody (1:200, ab97051, Abcam) or Goat Anti-Mouse IgG H&L (HRP) secondary antibody (1:2000, ab205719, Abcam) for 1 h at room temperature. Finally, 3, 3'-diaminobenzidine tetrahydrochloride (DAB) and hematoxylin staining were carried out. Images were captured under a microscope (Nikon, Tokyo, Japan). Image J software was used to determine OX-42, PPARγ and CD36 positive areas.

*Western blot analysis*

The brain tissues were treated with RIPA lysis buffer (Thermo, USA) to obtain total protein. The protein concentration was measured using a BSA kit (TaKaRa, Dalian). Then, approximately 20 μg protein was separated using 10% sodium dodecyl sulfate polyacrylamide gel electrophoresis and transferred onto a polyvinylidene fluoride (PVDF) membrane (Thermo Scientific, Madison, WI, USA). PVDF membranes were blocked with TBST solution containing 5% skim milk at room temperature for 3 h. The membranes were then incubated overnight with rabbit primary antibodies against PPARγ (1:1000, ab310323, Abcam), CD36 (1:1000, ab252922, Abcam), and beta-actin (1:1000, ab8227, Abcam) at 4°C followed by incubating with Goat Anti-Rabbit IgG H&L (HRP) secondary antibody (1:2000, ab97051, Abcam) for 1 h at room temperature. Finally, images were scanned and analyzed using a Quantity One Imaging System.

*qRT-PCR*

Total RNA was extracted from the brain tissues using TRIzol reagent (Invitrogen, USA). The first-strand cDNA was synthesized using the RevertAid First Strand

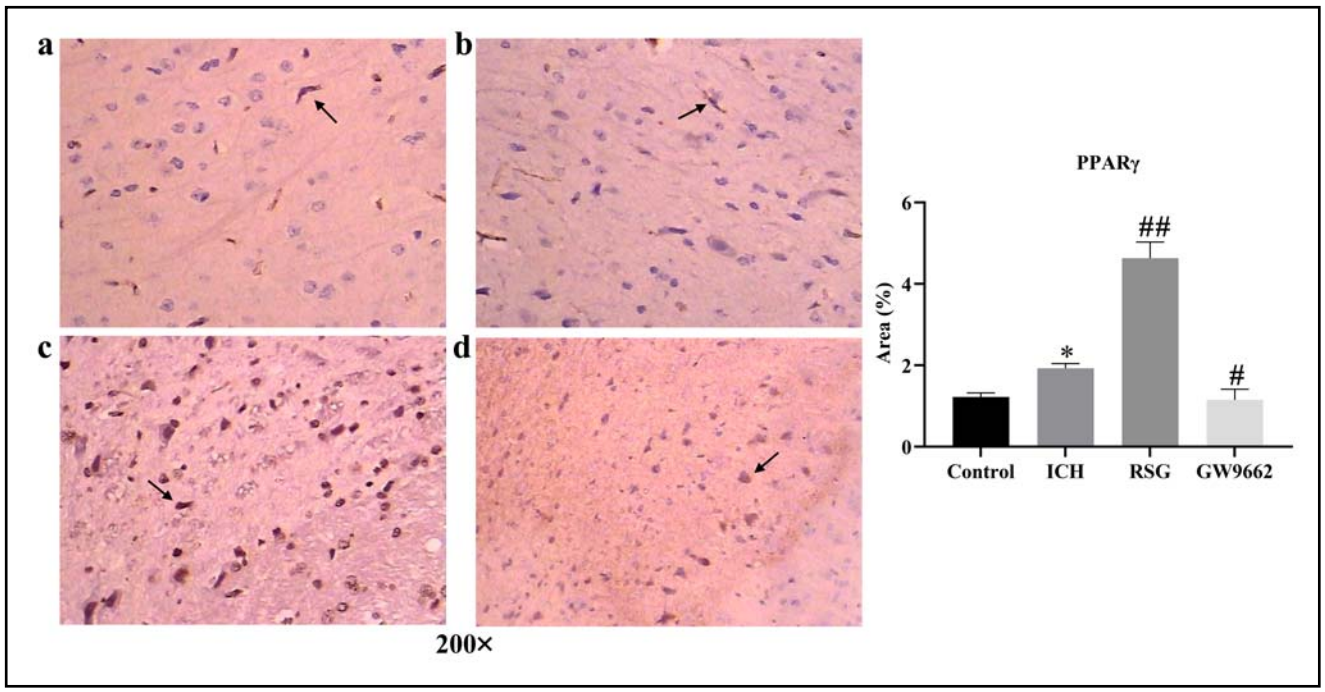


**Fig. 4. Expression of PPARγ in the surrounding tissues of each group 72 h after modeling.** (a) control group, (b) ICH group, (c) RSG group (PPARγ agonist group), (d) GW9662 group (PPARγ antagonist group). The arrow indicates PPARγ expression. Magnification: ×200. * $p < 0.05$ versus the control group. #$p < 0.05$ and ## $p < 0.01$ versus the ICH group.

cDNA synthesis kit (Thermo Fisher Scientific, MA, USA). qRT-PCR analyses of PPARγ and CD36 mRNAs were carried out on an ABI Q6 real-time PCR machine (Applied Biosystems Inc., MA, USA) using QuantiFast SYBR Green PCR Kit (Qiagen, Hilden, Germany). The PCR cycling parameters were: 95°C for 5 min, 40 cycles of 95°C for 10 s and 60°C for 30 s followed by a melting curve. Every sample was assayed in triplicates. The relative gene expression was determined using the $2^{-\Delta\Delta CT}$ method. All the primers were synthesized by Invitrogen (Beijing, China). Glyceraldehyde-3-phosphate dehydrogenase (GAPDH) was used as an internal control. The primers are displayed in Table S1.

*Statistical analysis*

All data were analyzed using the SPSS 17.0 software. The data were expressed as mean ± standard deviation. Statistical differences between more than two groups were assessed by one-way analysis of variance (ANOVA) followed by Tukey's multiple comparisons. $p < 0.05$ was considered statistically significant.

## RESULTS

*Characteristics of ICH model in rats*

We firstly constructed the ICH rat model and then verified whether the modeling was successful. As shown in Fig. S1, in the ICH rat model, the hematoma was formed in the right basal ganglia of the brain and generated a compression in the surrounding tissues. Even partial hematoma resulted in deviation of the midline. In addition, the brain tissues of the ICH rats were observed under the light microscope through HE staining. In the 6 h model group, cells in each layer of the brain tissue were closely arranged and had a complete structure. The nerve cells showed slight edema, the cytoplasm and core were evenly stained and the cell morphology was clear (Fig. 1a). In the 24 h model group, tissues around the hematoma were edematous, glial cells were swollen and the cell morphology was still clear (Fig. 1b). In the 48h model group, a large number of inflammatory cells were seen around the hematoma, glial cells and nerve cells were evidently swollen and a few nerve cells were necrotic (Fig. 1c). In the 72 h model group, the edema of the tissue cells was the most obvious. The interstitial space was also increased and some of the nerve cells were dead (Fig. 1d). These results indicated that the ICH rat model was successfully established.

*Rosiglitazone promotes the expression of OX-42, a microglial marker, in the brain tissues*

Immunohistochemistry was used to detect the expression of OX-42, a microglial marker, in the brain tissues after ICH. The number of OX-42 positive microglia was increased from 6 h to 72 h, indicating that the infiltration of microglia was enhanced (Fig. 2). In addition, the expression of OX-42 in the ICH group was statistically higher than that in the control group (Fig. 3a, 3b). Rosiglitazone pretreatment markedly increased OX-42 expression in the ICH rats (Fig. 3b, 3c), whereas GW9662 dramatically suppressed OX-42 expression in the ICH rats (Fig. 3b, 3d). These results revealed that rosiglitazone could promote microglial distribution around the hematoma.

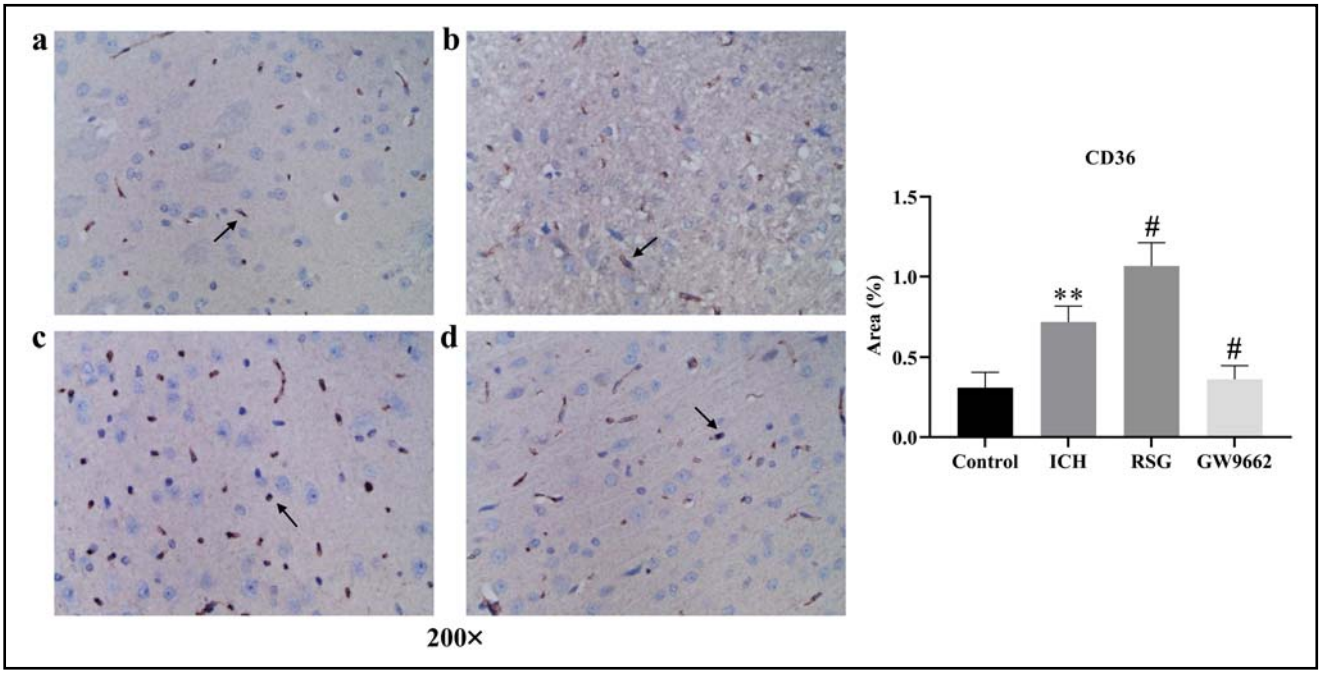


**Fig. 5. Expression of CD36 in the surrounding tissues of each group 72 h after modeling.** (a) control group, (b) ICH group, (c) RSG group (PPARγ agonist group), (d) GW9662 group (PPARγ antagonist group). The arrow indicates CD36 expression. Magnification: ×200. $^{**}p < 0.01$ versus the control group. $\#p < 0.05$ versus the ICH group.

*Rosiglitazone promotes the expression of PPARγ and CD36 around the hematoma after ICH*

The expression of PPARγ and CD36 around the hematoma was determined in all groups using immunohistochemical methods. The expression of PPARγ and CD36 were remarkably increased in the ICH group in comparison with the control group (Fig. 4a, 4b, 5a, 5b). After rosiglitazone stimulation, the expression of PPARγ and CD36 was significantly enhanced in the ICH rats (Fig. 4b, 4c, 5b, 5c). Conversely, after administration of GW9662, the expression of PPARγ and CD36 was significantly inhibited in the ICH rats (Fig. 4b, 4d, 5b, 5d).

*Rosiglitazone promotes the mRNA and protein expression of PPARγ and CD36 in the brain tissues*

The mRNA and protein expression levels of PPARγ in the brain tissues were detected at 6 h, 24 h, 48 h, and 72 h after ICH onset. The results showed that the mRNA and protein expression levels of PPARγ in the brain tissues were significantly increased at 48h and 72h after ICH (Fig. 6a, c). Rosiglitazone remarkably enhanced the mRNA and protein expression of PPARγ, but GW9662 had the opposite effect in brain tissues of ICH rats. Simultaneously, the mRNA and protein expression of CD36 in the brain tissues was also detected at 6 h, 24 h, 48 h, and 72 h after ICH onset. As shown in Fig. 6b and Fig. 6c, the mRNA and protein expression levels of CD36 were significantly enhanced after ICH (Fig. 6b, c). Additionally, rosiglitazone significantly promoted the mRNA and protein expression of CD36, whereas GW9662 did the opposite in brain tissues of ICH rats.

## DISCUSSION

Microglia are immune effector cells of the central nervous system, which belong to the mononuclear phagocyte system (Taylor & Sansing 2013). Under stress, microglia shift into M1 phenotypes, resulting in releasing inflammatory factors and promoting neuroinflammatory responses. After the inflammation fades away, microglia transform into M2 phenotypes and exert a role in neuroprotection (Zhang *et al.* 2018). They are closely related to the development of brain function and the stability of nervous system. Emerging evidence have confirmed that microglia activation plays a key role in secondary brain injury after ICH (Zhang *et al.* 2017; Wang & Dore 2007). Under normal conditions, microglia are in a static state. Once affected by changes in the external environment, they showed strong phagocytosis (Streit *et al.* 1999). Studies have shown that when the central nervous system is damaged or in a state of disease, microglia can achieve homeostasis by phagocytizing hematoma, promoting nervous system repair, and clearing toxic substances (Mammadov *et al.* 2012; Lull & Block 2010). Previous studies have shown that activated microglia enhanced the clearance of hematomas after ICH and promoted the recovery of neural function (Zhao *et al.* 2009; Xi *et al.* 2014). In our study, rosiglitazone remarkably enhanced the expression of OX-42, a microgial marker, around the hematoma in the ICH rat model. This confirmed that rosiglitazone could promote the microglial distribution to improve hematoma clearance.

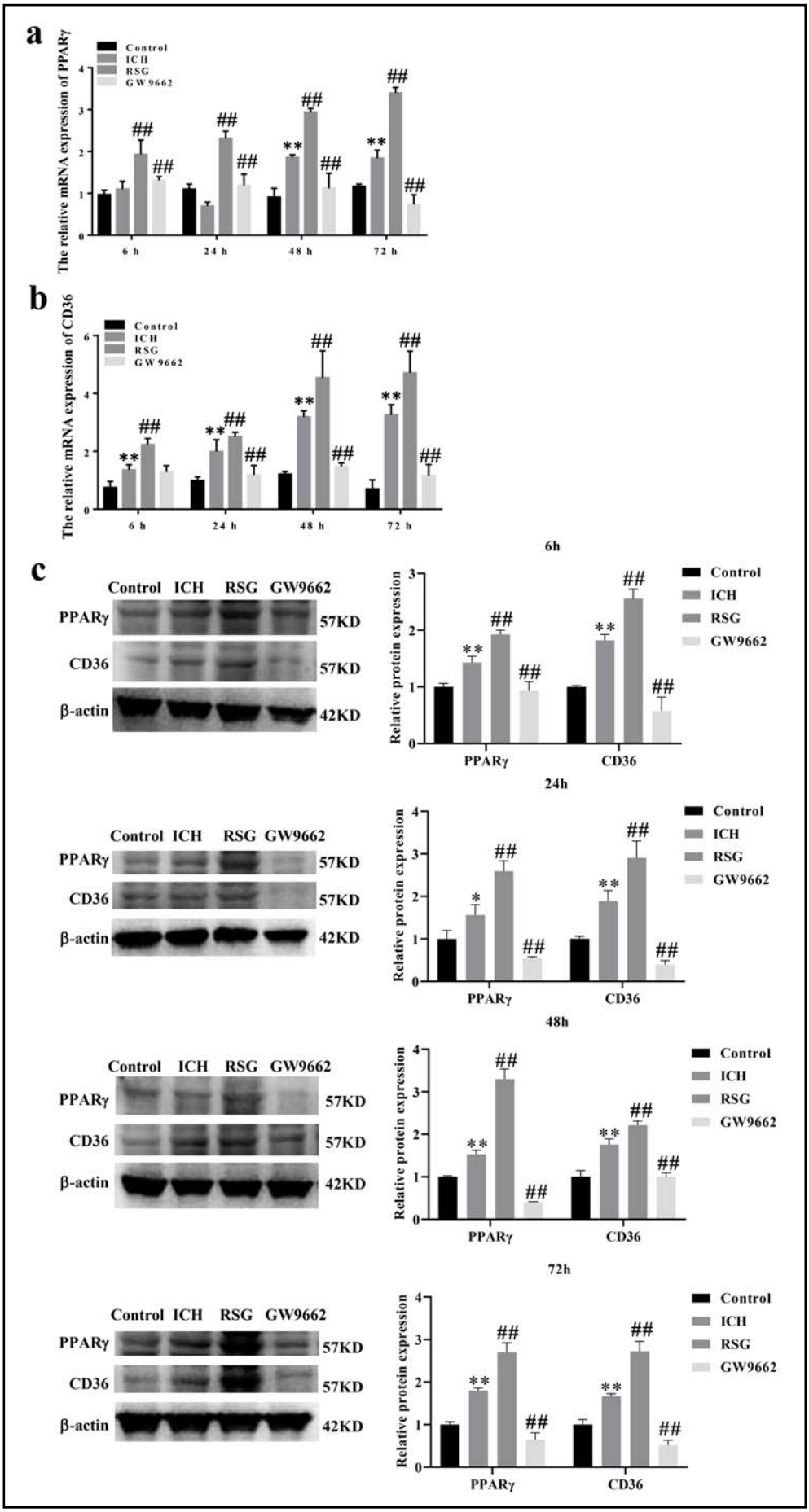


**Fig. 6. Relative mRNA and protein expression of PPARγ and CD36 in the brain tissues after ICH.** (a) Relative mRNA expression of PPARγ was detected by qRT-PCR. (b) Relative mRNA expression of CD36 was detected by qRT-PCR. (c) Protein expression of PPARγ and CD36 in different groups at 6 h, 24 h, 48 h and 72 h after modeling was determined by western blot. *$p < 0.05$ and ** $p < 0.01$ versus the control group. ## $p < 0.01$ versus the ICH group.

Recently, increasing evidence revealed that PPARγ participated in the activation of microglia/macrophages and reduction of oxidative stress and inflammation (Zhao *et al.* 2015; Gonzales *et al.* 2013). The neurological role of PPARγ agonists has been widely studied (Yu *et al.* 2008). Studies in animal models of ICH showed that PPARγ agonists inhibited the release of pro-inflammatory mediators produced by microglia/macrophages (such as, IL-1β, iNOS, and TNF-α), while increased the levels of anti-inflammatory cytokines (such as, IL-10, TGF-β, etc.) (Standiford *et al.* 2005; Zhao *et al.* 2016). In vitro, PPARγ agonists interfere with inflammatory responses in the process of microglial activation (Ricote *et al.* 1998; Park *et al.* 2003). PPARγ agonists exert a crucial role in transition of microglial phenotypes and neuroprotection. Pioglitazone alleviated cognitive deficits in male rat offspring via PPARγ-dependent regulation of microglial phenotypes (Han *et al.* 2020). In addition, PPARγ is expressed in microglia and PPARγ activation in microglia may modulate the phenotypic change of microglia (Wen *et al.* 2018). Rosiglitazone, which has PPARγ activating ability, regulates microglia indirectly. Krishna *et al.* found that PPAR-γ activation by rosiglitazone enhanced microglial phagocytic activity (Krishna *et al.* 2021). Song *et al.* investigated the mechanism of rosiglitazone against secondary brain injury caused by cerebral hemorrhage and revealed that rosiglitazone could raise the thrombin-induced antioxidative ability of microglia (Song *et al.* 2018). Wu *et al.* found that rosiglitazone enhanced perihematomal PPARγ levels. They also found that after rosiglitazone was infused into the hematoma area, it mitigated blood-brain barrier (BBB) disruption, thereby effectively lowering secondary injury to the brain and improving neurological function in rabbits (Wu *et al.* 2016). In accordance with these results, in this study, rosiglitazone significantly promoted the mRNA and protein expression levels of PPARγ in ICH rats.

CD36 is widely present in microglia, platelets, and vascular endothelial cells (Silverstein & Febbraio 2009). Activated-microglia can recognize and phagocytize erythrocytes through the scavenger receptor CD36 after ICH (Jesberger & Richardson 1991). The previous study has demonstrated that CD36 could mediate hematoma absorption (Fernandezlopez *et al.* 2016; Serghides 2012). CD36 can be regulated by PPARγ (Zhao *et al.* 2009). Rosiglitazone-induced CD36 increase resolves inflammation via the PPARγ pathway (Ballesteros *et al.* 2013). Another study has reported that activation of PPARγ could help activate microglia to remove necrotic or apoptotic cells by up-regulating the expression of CD36 on the cell surface (Flores *et al.* 2016). Consistent with these findings, in our study, we discovered that rosiglitazone dramatically increased CD36 expression in the ICH rats.

The neuroprotective effects of microglia on ICH through the PPARγ/CD36 pathway has been reported. For example, wogonin improved neurological recovery after ICH by promoting the expression of Axl, MerTK, CD36, and LAMP2 in microglia through the PPAR-γ pathway (Zhuang *et al.* 2021). Vitamin D facilitated hematoma clearance after ICH and enhanced the levels of CD36 and PPAR-γ in the brain (Liu *et al.* 2022). ISO-alpha-acids improved ICH performance by transforming microglia through the PPARγ-CD36 pathway in ICH rats (Zhao *et al.* 2020). Thus, we speculated that rosiglitazone promotes microglial distribution via activation of PPARγ and CD36 through the PPARγ pathway.

In summary, our study demonstrated that rosiglitazone could regulate the microglial distribution around the hematoma in the ICH rat model and promote the expression of PPARγ and CD36 through the PPARγ pathway. Our findings offer novel insights into the mechanism by which rosiglitazone promotes microglial distribution after ICH.

## ACKNOWLEDGEMENTS

Not applicable.

## FUNDING

This work was supported by the Science and Technology Fund project of Guizhou Provincial Health Commission (gzwkj2021-030) and National Natural Science Foundation of China (81971126/H0906).

## CONFLICT OF INTEREST

The authors declared that they have no conflict of interest.

## ETHICS APPROVAL

All experimental procedures were approved by the Ethical Committee and the Animal Experimental Committee of Guizhou Medical University.

## AVAILABILITY OF DATA AND MATERIALS

The datasets used and/or analyzed during the current study are available from the corresponding author on reasonable request.

## AUTHORS' CONTRIBUTIONS

Conceptualization: GW. Data curation: QH. Methodology: HZ, YX. Experiments and Writing-original draft: QM. Writing-review & editing: QM, GW. All authors read and approved the final manuscript.

REFERENCES

1 Ballesteros I, Cuartero MI, Pradillo JM, De La Parra J, Perez-Ruiz A, Corbi A, et al. (2013). Rosiglitazone-induced CD36 up-regulation resolves inflammation by PPAR and 5-LO-dependent pathways. Journal of Leukocyte Biology. **95**: 587–598.

2 Berger J, Moller DE (2002). The mechanisms of action of PPARs. Annu Rev Med. **53**: 409–435.
3 De Oliveira MA (2020). Surgery for spontaneous intracerebral hemorrhage. Critical care (London, England). **24**: 45.
4 Duan X, Wen Z, Shen H, Shen M, Chen G (2016). Intracerebral Hemorrhage, Oxidative Stress, and Antioxidant Therapy. Oxidative medicine and cellular longevity. **2016**: 1203285.
5 Fadok VA, Warner ML, Bratton DL, Henson PM (1998). CD36 is required for phagocytosis of apoptotic cells by human macrophages that use either a phosphatidylserine receptor or the vitronectin receptor (αvβ3). The Journal of Immunology. **161**: 6250–6257.
6 Fang H, Chen J, Lin S, Wang P, Wang Y, Xiong X, et al. (2014). CD36-mediated hematoma absorption following intracerebral hemorrhage: negative regulation by TLR4 signaling. J Immunol. **192**: 5984–5992.
7 Fei X, He Y, Chen J, Man W, Chen C, Sun K, et al. (2019). The role of Toll-like receptor 4 in apoptosis of brain tissue after induction of intracerebral hemorrhage. J Neuroinflammation. **16**: 234.
8 Fernandezlopez D, Faustino J, Klibanov AL, Derugin N, Blanchard E, Simon F, et al. (2016). Microglial Cells Prevent Hemorrhage in Neonatal Focal Arterial Stroke. The Journal of Neuroscience. **36**: 2881–2893.
9 Fischer M, Schiefecker AJ, Lackner P, Frank F, Helbok R, Beer R, et al. (2017). Targeted Temperature Management in Spontaneous Intracerebral Hemorrhage: A Systematic Review. Current Drug Targets. **18**: 1430–1440.
10 Flores J, Klebe D, Rolland W, Lekic T, Krafft P, Zhang J (2016). PPARγ-induced upregulation of CD36 enhances hematoma resolution and attenuates long-term neurological deficits after germinal matrix hemorrhage in neonatal rats. Neurobiology of disease. **87**: 124–133.
11 Gonzales N, Shah J, Sangha N, Sosa L, Martinez R, Shen L, Kasam M, Morales M, et al. (2013). Design of a prospective, dose-escalation study evaluating the Safety of Pioglitazone for Hematoma Resolution in Intracerebral Hemorrhage (SHRINC). International journal of stroke: official journal of the International Stroke Society. **8**: 388–396.
12 Han N, Ding S, Wu T, Zhu Y (2008). Correlation of free radical level and apoptosis after intracerebral hemorrhage in rats. Neuroscience Bulletin. **24**: 351–358.
13 Han Y, Wang J, Zhao Q, Xie X, Song R, Xiao Y, Kang X, Zhang L, et al. (2020). Pioglitazone alleviates maternal sleep deprivation-induced cognitive deficits in male rat offspring by enhancing microglia-mediated neurogenesis. Brain, behavior, and immunity. **87**: 568–578.
14 Jesberger JA, Richardson JS (1991). Oxygen Free Radicals and Brain Dysfunction. International Journal of Neuroscience. **57**: 1–17.
15 Keep RF, Hua Y, Xi G (2012). Intracerebral haemorrhage: mechanisms of injury and therapeutic targets. Lancet Neurology. **11**: 720–731.
16 Kirkman MA, Allan SM, Parry-Jones AR (2011). Experimental intracerebral hemorrhage: avoiding pitfalls in translational research. J Cereb Blood Flow Metab. **31**: 2135–2151.
17 Kisa A, Kisa S, Collaborators GS (2021). Global, regional, and national burden of stroke and its risk factors, 1990–2019: a systematic analysis for the Global Burden of Disease Study 2019. The Lancet Neurology: **26**.
18 Kollmar R, Juettler E, Huttner HB, Dorfler A, Staykov D, Kallmuenzer B, et al. (2012). Cooling in intracerebral hemorrhage (CINCH) trial: protocol of a randomized German-Austrian clinical trial. International Journal of Stroke. **7**: 168–172.
19 Krishna S, Cheng B, Sharma DR, Yadav S, Stempinski ES, Mamtani S, et al. (2021). PPAR-γ activation enhances myelination and neurological recovery in premature rabbits with intraventricular hemorrhage. Proceedings of the National Academy of Sciences. **118**: e2103084118.
20 Lan X, Han X, Li Q, Yang Q, Wang J (2017). Modulators of microglial activation and polarization after intracerebral haemorrhage. Nature reviews Neurology. **13**: 420–433.
21 Liu J, Li N, Zhu Z, Kiang KM, Ng ACK, Dong CM, et al. (2022). Vitamin D Enhances Hematoma Clearance and Neurologic Recovery in Intracerebral Hemorrhage. Stroke. **53**: 2058–2068.
22 Lull ME, Block ML (2010). Microglial Activation & Chronic Neurodegeneration. Neurotherapeutics. **7**: 354–365.
23 Mammadov E, Aridogan IA, Izol V, Acikalin A, Abat D, Tuli A, et al. (2012). Protective Effects of Phosphodiesterase-4-specific Inhibitor Rolipram on Acute Ischemia-reperfusion Injury in Rat Kidney. Urology. **80**: 1390.e1391–1390.e1396.
24 Park EJ, Park SY, Joe E, Jou I (2003). 15d-PGJ2 and rosiglitazone suppress Janus kinase-STAT inflammatory signaling through induction of suppressor of cytokine signaling 1 (SOCS1) and SOCS3 in glia. Journal of Biological Chemistry. **278**: 14747–14752.
25 Qureshi A, Palesch Y, Barsan W, Hanley D, Hsu C, Martin R, et al. (2016). Intensive Blood-Pressure Lowering in Patients with Acute Cerebral Hemorrhage. The New England journal of medicine. **375**: 1033–1043.
26 Qureshi A, Qureshi M (2018). Acute hypertensive response in patients with intracerebral hemorrhage pathophysiology and treatment. Journal of cerebral blood flow and metabolism : official journal of the International Society of Cerebral Blood Flow and Metabolism. **38**: 1551–1563.
27 Ricote M, Li A, Willson T, Kelly C, Glass C (1998). The peroxisome proliferator-activated receptor-gamma is a negative regulator of macrophage activation. Nature.
28 Sagir D, Eren B, Yilmaz BD, Eren Z, Keles ON, Gokce AB (2018). Effects of prenatal PPAR-gamma agonist rosiglitazone exposure on rat hippocampus development in a time-dependent manner: A stereological and histopathological study. Human & experimental toxicology. **37**: 827–835.
29 Serghides L (2012). The Case for the Use of PPARγ Agonists as an Adjunctive Therapy for Cerebral Malaria. Ppar Research. **2012**: 513865–513865.
30 Silverstein RL, Febbraio M (2009). CD36, a Scavenger Receptor Involved in Immunity, Metabolism, Angiogenesis, and Behavior. Science Signaling. **2**.
31 Song A, Wu G, Hang H, Wang L (2018). Rosiglitazone pretreatment influences thrombin-induced anti-oxidative action via activating NQO1and γ-GCS in rat microglial cells. Neurological Research. **40**: 139–145.
32 Standiford TJ, Keshamouni VG, Reddy RC (2005). Peroxisome proliferator-activated receptor-{gamma} as a regulator of lung inflammation and repair. Proc Am Thorac Soc. **2**: 226–231.
33 Streit WJ, Walter SA, Pennell NA (1999). Reactive microgliosis. Progress in Neurobiology. **57**: 563–581.
34 Sundararajan S, Jiang Q, Heneka M, Landreth G (2006). PPARγ as a therapeutic target in central nervous system diseases. Neurochemistry international. **49**: 136–144.
35 Taylor RA, Sansing LH (2013). Microglial Responses after Ischemic Stroke and Intracerebral Hemorrhage. Clinical & Developmental Immunology. **2013**: 746068–746068.
36 Wang J (2010). Preclinical and clinical research on inflammation after intracerebral hemorrhage. Progress in neurobiology. **92**: 463–477.
37 Wang J, Dore S (2007). Inflammation after intracerebral hemorrhage. Journal of cerebral blood flow and metabolism: official journal of the International Society of Cerebral Blood Flow and Metabolism. **27**: 894–908.
38 Wang L, Liu W, Fan Y, Liu T, Yu C (2017). Effect of rosiglitazone on amyloid precursor protein processing and Aβ clearance in streptozotocin-induced rat model of Alzheimer's disease. Iranian Journal of Basic Medical Sciences. **20**: 474–480.
39 Wen L, You W, Wang H, Meng Y, Feng J, Yang X (2018). Polarization of Microglia to the M2 Phenotype in a Peroxisome Proliferator-Activated Receptor Gamma-Dependent Manner Attenuates Axonal Injury Induced by Traumatic Brain Injury in Mice. Journal of neurotrauma. **35**: 2330–2340.
40 Wu G, Wu J, Jiao Y, Wang L, Wang F, Zhang Y (2015). Rosiglitazone infusion therapy following minimally invasive surgery for intracerebral hemorrhage evacuation decreases matrix metalloproteinase-9 and blood–brain barrier disruption in rabbits. BMC Neurology. **15**: 37–37.
41 Wu G, Wu J, Wang L, Jiao Y, Zhou H, Tang Z (2016). Minimally invasive surgery for ICH evacuation followed by rosiglitazone infusion therapy increased perihematomal PPARγ expression and improved neurological outcomes in rabbits. Neurological Research. **38**: 261–268.

42 Xi G, Strahle J, Hua Y, Keep RF (2014). Progress in translational research on intracerebral hemorrhage: Is there an end in sight? Progress in Neurobiology. **115**: 45–63.

43 Xiao H, Liu J, He J, Lan Z, Deng M, Hu Z (2021). 17beta-Estradiol Attenuates Intracerebral Hemorrhage-Induced Blood-Brain Barrier Injury and Oxidative Stress Through SRC3-Mediated PI3K/Akt Signaling Pathway in a Mouse Model. ASN Neuro. **13**: 17590914211038443.

44 Yao J, Zheng K, Zhang X (2015). Rosiglitazone exerts neuroprotective effects via the suppression of neuronal autophagy and apoptosis in the cortex following traumatic brain injury. Mol Med Rep. **12**: 6591–6597.

45 Yu X, Shao X, Sun H, Li Y, Yang J, Deng Y, et al. (2008). Activation of cerebral peroxisome proliferator-activated receptors gamma exerts neuroprotection by inhibiting oxidative stress following pilocarpine-induced status epilepticus. Brain research. **1200**: 146–158.

46 Zhang J, Dong B, Hao J, Yi S, Cai W, Luo Z (2019). LncRNA Snhg3 contributes to dysfunction of cerebral microvascular cells in intracerebral hemorrhage rats by activating the TWEAK/Fn14/STAT3 pathway. Life Sci. **237**: 116929.

47 Zhang L, Wang L, Xiao H, Gan H, Chen H, Zheng S, et al. (2021). Tyrosine kinase Fyn promotes apoptosis after intracerebral hemorrhage in rats by activating Drp1 signaling. J Mol Med (Berl). **99**: 359–371.

48 Zhang L, Zhang J, You Z (2018). Switching of the Microglial Activation Phenotype Is a Possible Treatment for Depression Disorder. Front Cell Neurosci. **12**: 306.

49 Zhang Z, Zhang Z, Lu H, Yang Q, Wu H, Wang J (2017). Microglial Polarization and Inflammatory Mediators After Intracerebral Hemorrhage. Mol Neurobiol. **54**: 1874–1886.

50 Zhao JL, Chen YJ, Yu J, Du ZY, Yuan Q, Sun YR, et al. (2020). ISO-alpha-acids improve the hematoma resolution and prevent perihematoma inflammations by transforming microglia via PPARgamma-CD36 axis in ICH rats. International immunopharmacology. **83**: 106396.

51 Zhao Q, Wu X, Yan S, Xie X, Fan Y, Zhang J, et al. (2016). The antidepressant-like effects of pioglitazone in a chronic mild stress mouse model are associated with PPARγ-mediated alteration of microglial activation phenotypes. Journal of Neuroinflammation. **13**: 259–259.

52 Zhao X, Gonzales N, Aronowski J (2015). Pleiotropic role of PPARγ in intracerebral hemorrhage: an intricate system involving Nrf2, RXR, and NF-κB. CNS neuroscience & therapeutics. **21**: 357–366.

53 Zhao X, Grotta JC, Gonzales NR, Aronowski J (2009). Hematoma Resolution as a Therapeutic Target The Role of Microglia/Macrophages. Stroke. **40**.

54 Zhao X, Sun G, Zhang J, Strong R, Song W, Gonzales N, et al. (2007). Hematoma resolution as a target for intracerebral hemorrhage treatment: Role for peroxisome proliferator-activated receptor γ in microglia/macrophages. Annals of Neurology. **61**: 352–362.

55 Zhuang J, Peng Y, Gu C, Chen H, Lin Z, Zhou H, et al. (2021). Wogonin Accelerates Hematoma Clearance and Improves Neurological Outcome via the PPAR-gamma Pathway After Intracerebral Hemorrhage. Translational stroke research. **12**: 660–675.

## SUPPLEMENTARY FILES

**Supp. Tab. 1.** Sequences of forward and reverse primers used in the qRT-PCR experiment

| Gene name | Primers name | Primers sequence |
|---|---|---|
| PPARγ | PPARγ-F | 5′- TACCACGGTTGATTTCTC -3′ |
| | PPARγ-R | 5′-GCTCTACTTTGATCGCACT -3′ |
| CD36 | CD36-F | 5′- ATGAGACTGGGACCATCGGC -3′ |
| | CD36-R | 5′-CAACAAACATCACTACTCCAACACC -3′ |
| GAPDH | GAPDH-F | 5′-CCTTCCGTGTTCCTACCCC-3′ |
| | GAPDH-R | 5′-GCCCAGGATGCCCTTTAGTG-3′ |

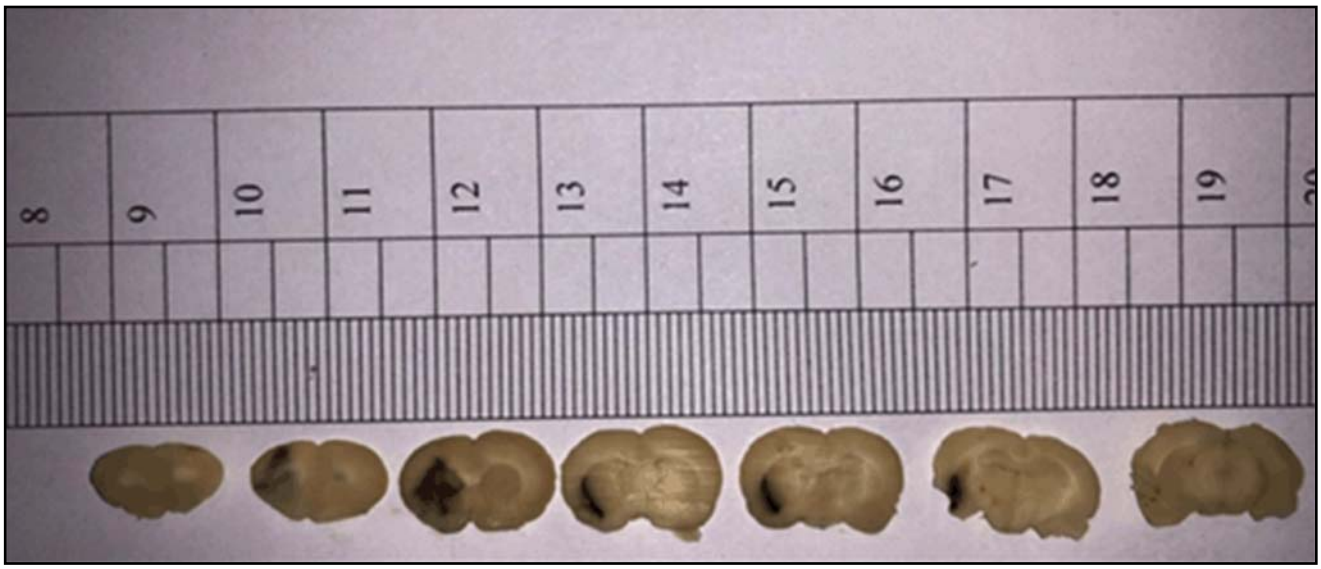


**Supp. Fig. 1.** Coronal profile of the brain tissues in the ICH rat model.